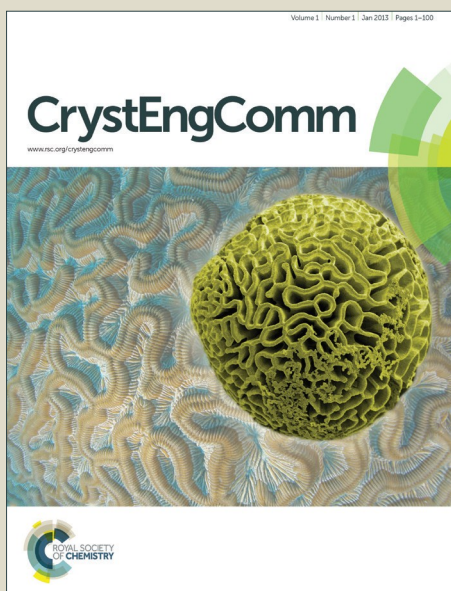


CrystEngComm

Accepted Manuscript



This is an *Accepted Manuscript*, which has been through the Royal Society of Chemistry peer review process and has been accepted for publication.

Accepted Manuscripts are published online shortly after acceptance, before technical editing, formatting and proof reading. Using this free service, authors can make their results available to the community, in citable form, before we publish the edited article. We will replace this *Accepted Manuscript* with the edited and formatted *Advance Article* as soon as it is available.

You can find more information about *Accepted Manuscripts* in the [Information for Authors](#).

Please note that technical editing may introduce minor changes to the text and/or graphics, which may alter content. The journal's standard [Terms & Conditions](#) and the [Ethical guidelines](#) still apply. In no event shall the Royal Society of Chemistry be held responsible for any errors or omissions in this *Accepted Manuscript* or any consequences arising from the use of any information it contains.

**From single-point to three-point halogen bonding between
zinc(II) tetrathiocyanate and tetrabromomethane.[†]**

Sergiy V. Rosokha,^{a,*} Charlotte L. Stern,^b and Michael K. Vinakos^{a,‡}

^a*Department of Biological, Chemical and Physical Sciences, Roosevelt University, Chicago IL 60605*

^b*Department of Chemistry, Northwestern University, Evanston, Illinois 60208*

E-mail: srosokha@roosevelt.edu

Abstract

X-ray structural analysis revealed that $(\text{Bu}_4\text{N})_2[\text{Zn}(\text{NCS})_4] \cdot 3\text{CBr}_4$ co-crystals comprise a honeycomb-like network in which each thiocyanate anion is linked to the zinc(II) cation via N-Zn coordination bond and to three tetrabromomethane molecules via $\text{S} \cdots \text{Br}$ halogen bonds. Most of the halogen bonds in this hybrid network are similar to those between the CBr_4 molecules and the separate NCS^- anions. However, it also contains unusual two-point interaction involving two NCS^- ligands of the $[\text{Zn}(\text{NCS})_4]^{2-}$ complex and two bromine substituents of the CBr_4 molecule. DFT computations with the ωB97XD and M062X functionals confirmed that the two-point-bonded complex represents a (local) energy minimum for the $\text{CBr}_4 \cdot [\text{Zn}(\text{NCS})_4]^{2-}$ dyads. These computations also revealed that complexes in which $[\text{Zn}(\text{NCS})_4]^{2-}$ dianion and CBr_4 molecule are linked by three-point halogen bonds are characterized by somewhat lower energy both in the gas phase and in dichloromethane. Yet, the strengths of these two- and three-point halogen bonds are close to that between the CBr_4 molecule and the NCS^- anion (and experimental formation constants of $\text{CBr}_4 \cdot [\text{Zn}(\text{NCS})_4]^{2-}$ and $\text{CBr}_4 \cdot \text{NCS}^-$ associates in dichloromethane are also similar). This indicates that each component of the multicenter interaction is significantly weaker than the one-point $\text{CBr}_4 \cdot \text{NCS}^-$ halogen bond. The lack of the enhancement of the strength of multi-point bonding is apparently related to the deviations of the geometries of individual halogen bonds involved in these multicenter interactions from their optimal values.

[†]Electronic supplementary information (ESI) available: Energies and atomic coordinates of the calculated complexes, crystal structure details. CCDC 1421337. For ESI and crystallographic data in CIF or other electronic format see DOI:

[‡] Current address: Particle Technology Labs, Downers Grove, IL, 606015

Introduction.

Combination of metal complexes with organic molecules in metal-organic networks appeared recently as an efficient method for preparation of high-performance and tunable materials with interesting magnetic and optical properties, solid-state frameworks for storage of gases, catalysis, and a variety of other applications.^{1,2} During the last decade, a number of publications have shown that formation of such hybrid networks can be facilitated by halogen bonding, the highly directional attraction between electrophilic halogen substituents in organic molecules and electron-rich sites (such as metal-coordinated anions).^{3,4}

Pseudohalide (e.g. NCS^- or N_3^-) anions appear as one of the most promising types of ligands for preparation of the networks based on the combination of coordination and halogen bonding. First, due to their “flexidentate” nature and bridging capacities with regard to metal-ion coordination, these anions are known as effective building blocks in crystal engineering and material science, and they have been frequently used as crystallizing agents in protein crystallography.^{5,6} Second, several publications demonstrated that these anions are efficient halogen-bond acceptors that form 1:1 complexes with halogenated electrophiles in solutions and 2D- and 3D-networks in the solid state.⁷⁻¹² Furthermore, X-ray structural and computational analyses of the intermolecular associates involving thiocyanate and cyanate anions established the polydentate nature of these pseudohalides with regard to halogen bonding.^{10,12} Yet, most of the studies of halogen-bonded metal-organic systems were focused on the halometallates which formed halogen-bonded networks with their cationic (e. g. halopyridinium) counter-ions or co-crystals with the neutral organic electrophiles.¹³⁻¹⁵ Besides earlier published structures in which short contacts between diiodine or iodoform and metal-coordinated thiocyanate can be identified,¹⁶ the data on the halogen bonding involving pseudohalide ligands are limited mostly

to structural characterization of cyanometallates with halogen-substituted pyridinium counter-ions and metal-coordinated thiocyanate with partially oxidized iodotetrathiafulvalenes.¹⁷ In these systems, halogen bonding is facilitated (and might be considerably affected) by the electrostatic attraction between anionic and cationic counter-parts. Furthermore, there is essentially no data which would allow direct comparison of the characteristics of the halogen bond between the same halogen-bond donor with the metal-coordinated and the separate halogen-bond acceptors.

The goal of the current work is to characterize halogen bonding of the metal-coordinated thiocyanate anions with halogenated electrophiles in solution and in the solid state and to establish how the presence of metal ions affects halogen bonding. This study will focus on the interaction between zinc tetrathiocyanate dianion, $[\text{Zn}(\text{NCS})_4]^{2-}$, and tetrabromomethane, CBr_4 . These molecules are transparent in most of the UV-Vis range, which facilitates spectrophotometric measurements of their interaction in solution. In addition, the spectral, thermodynamic, and structural features of the halogen-bonded associates between CBr_4 and the separate thiocyanate anion are available in the literature.^{8, 12} Thus, the comparison of the characteristics of halogen bonds in the presence of the metal ion and in its absence will clarify the effects of coordination on halogen bonding involving this anionic ligand. Finally, the availability of several centers suitable for halogen bonding in both tetrabromomethane and in the $[\text{Zn}(\text{NCS})_4]^{2-}$ complex allows the exploration of a variety of interaction modes between these polydentate halogen-bond donors and acceptors.

Results and Discussion.

UV-Vis spectroscopic measurements demonstrated that addition of zinc tetrathiocyanate to a solution of tetrabromomethane in dichloromethane resulted in formation of a complex with an absorption band at $\lambda_{\max} = 280$ nm (Figure 1). This band is significantly blue shifted as compared to the analogous absorption band at $\lambda_{\max} = 315$ nm of the CBr_4 complex with the separate (uncoordinated) thiocyanate anion, $\text{CBr}_4 \cdot \text{NCS}^-$.⁸ The treatment of the dependence of the intensity of the band at 280 nm on concentrations of CBr_4 and $(\text{Bu}_4\text{N})_2 [\text{Zn}(\text{NCS})_4]$ resulted in a formation constant of the $\text{CBr}_4 \cdot [\text{Zn}(\text{NCS})_4]^{2-}$ associate of about 0.8 M^{-1} (see the Experimental section for the details), which is similar to the earlier reported value for the $\text{CBr}_4 \cdot \text{NCS}^-$ complex.⁸

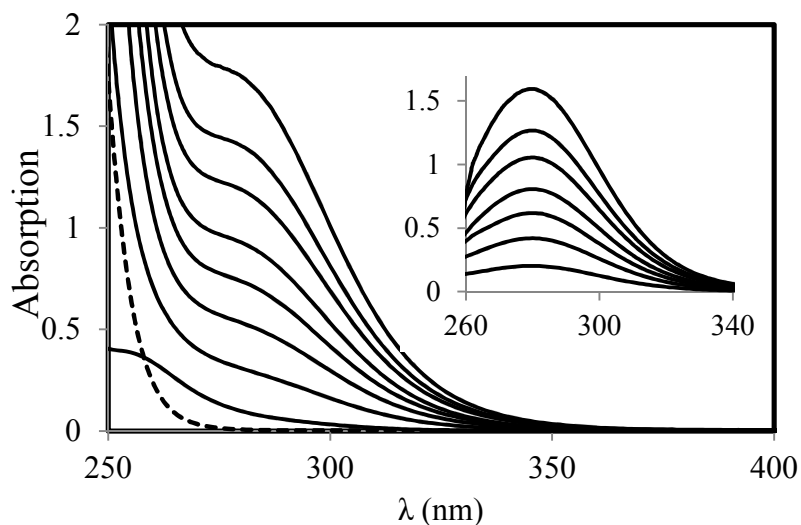


Figure 1. Spectral changes resulting from the addition of $(\text{Bu}_4\text{N})_2 [\text{Zn}(\text{NCS})_4]$ to 3.4 mM solution of CBr_4 in dichloromethane (19 °C). Concentration of $(\text{Bu}_4\text{N})_2 [\text{Zn}(\text{NCS})_4]$ (in mM, solid lines from the bottom to the top at 280 nm): 0, 64, 128, 192, 255, 316, 383, and 510. Dashed line represents spectrum of the separate 66 mM solution of $(\text{Bu}_4\text{N})_2 [\text{Zn}(\text{NCS})_4]$. Insert: Absorption spectra of $\text{CBr}_4 \cdot [\text{Zn}(\text{NCS})_4]^{2-}$ associate obtained by subtraction of the absorption of components from the spectra of their mixtures.

An analogous blue-shift of the absorption band of the associates between tetrabromomethane and tetrabromozincate as compared to those of $\text{CBr}_4 \cdot \text{Br}^-$ complex was observed previously.¹⁴ The higher absorption bands' energies of the $\text{CBr}_4 \cdot [\text{Zn}(\text{NCS})_4]^{2-}$ and

$\text{CBr}_4 \cdot [\text{ZnBr}_4]^{2-}$ associates are apparently related to the lower energies of the highest occupied molecular orbitals of these zinc complexes as compared to those of the separate halide or pseudohalide anions.¹⁸

Diffusion of hexane into a dichloromethane solution containing tetrabromomethane and the tetrabutylammonium salt of zinc tetrathiocyanate resulted in the formation of colorless crystals suitable for the X-ray crystallographic measurements (see Experimental for the details). The asymmetric unit of these (rod-like) crystal contains the $[\text{Zn}(\text{NCS})_4]^{2-}$ dianion and Bu_4N^+ counterions, as well as three crystallographically independent CBr_4 molecules (Figure 2).

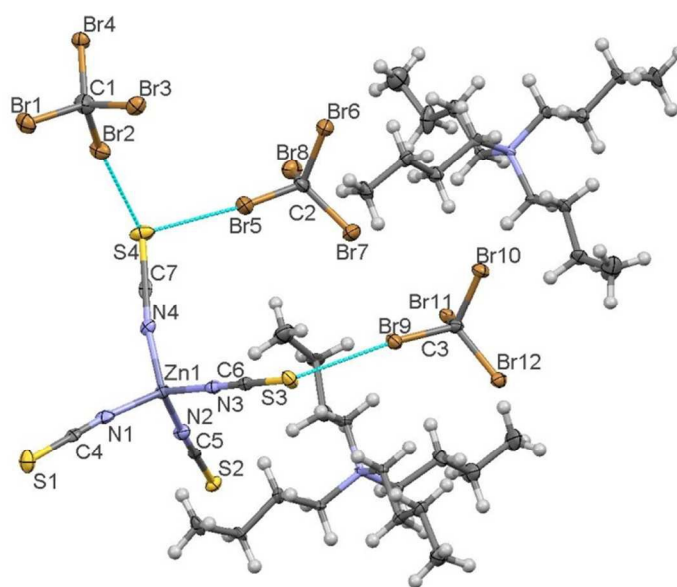


Figure 2. The asymmetric unit and atom numbering in the $(\text{Bu}_4\text{N})_2[\text{Zn}(\text{NCS})_4] \cdot 3\text{CBr}_4$ co-crystals. Blue lines show contacts between thiocyanate and tetrabromomethane shorter than the sum of the van der Waals radii of sulfur and bromine. Ellipsoids are shown at 50%, hydrogen atoms are drawn as fixed-size spheres. (Note: atom numbering in the tetrabutylammonium counter-ions is omitted, for clarity).

The nearly linear thiocyanate ligands (average N-C-S angle is 179.1 ± 0.7 deg) are characterized by the average carbon-sulfur bond length of 1.627 ± 0.012 Å, which is close to the typical

C=S double bond of 1.61 Å. The average carbon-nitrogen bond length of 1.153 ± 0.007 Å in these anions is midway between N=C double bond of 1.22 Å and N≡C triple bond of 1.11 Å). Each thiocyanate ligand is coordinated to the zinc ion via its nitrogen atom and its sulfur end shows three short intermolecular contacts with the bromine substituents of CBr₄ molecules (Figure 3).

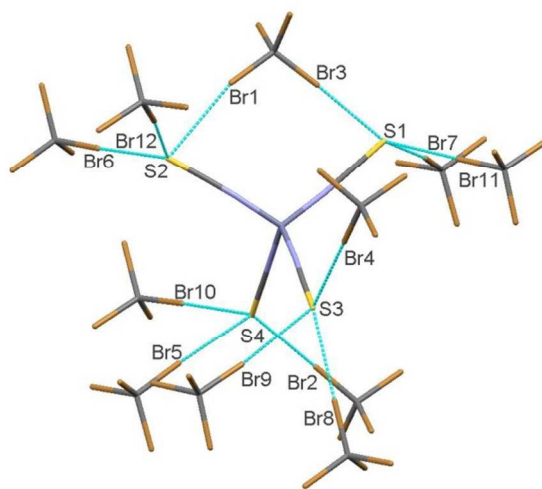


Figure 3. Halogen bonds (shown as light blue lines) between zinc thiocyanate and tetrabromomethane in the $(\text{Bu}_4\text{N})_2[\text{Zn}(\text{NCS})_4] \cdot 3\text{CBr}_4$ co-crystals. Symmetry codes: Br10: (1-x, -1/2+y, 1+z); Br4: (x,y,1+z); Br8: (1-x, 1/2+y, 1-z); Br1: (-x, -1/2+y, 1-z); Br6: (1-x, -1/2+y, 1-z); Br12: (1-x, -1/2+y, 2-z); Br7: (-1+x, y, z); Br11: (-1+x, y, z).

In turn, each tetrabromomethane form four short contacts (via its bromine substituents) with sulfur atoms of four thiocyanate ligands. The S...Br contact are 6 - 15 % shorter as compared to the sum of the van der Waals radii of interacting atoms of 3.65 \AA^{19} and most of the C-Br...S angles are in the 168 to 178 deg range. Such contractions of interatomic distances and near linear C-X...D angles are typical for halogen-bonded complexes. The geometric characteristics of these twelve crystallographically-independent halogen bonds are listed in Table 1.

Table 1. Characteristics of halogen bonds in the $(\text{Bu}_4\text{N})_2[\text{Zn}(\text{NCS})_4]\cdot 3\text{CBr}_4$ co-crystals.

Contact	$d_{\text{Br}\cdots\text{S}}$, Å	$\angle\text{C-Br}\cdots\text{S}$, deg	$\angle\text{C-S}\cdots\text{Br}$, deg
S4...Br2	3.2239(15)	167.78(18)	122.82(17)
S4...Br5	3.2788(15)	175.38(13)	107.54(15)
S4...Br10 ⁱ	3.1700(16)	177.83(13)	121.50(19)
S3 ... Br4 ⁱⁱ	3.2064(14)	173.62(15)	97.52(16)
S3 ... Br8 ⁱⁱⁱ	3.3488(15)	179.03(15)	128.48(16)
S3 ... Br9	3.3583(13)	174.01(13)	115.97(16)
S2... Br1 ^{iv}	3.4249(13)	158.90(17)	78.78(16)
S2... Br6 ^v	3.2658(14)	177.12(15)	122.06(17)
S2... Br12 ^{vi}	3.2379(13)	174.95(13)	121.56(17)
S1... Br3 ^{iv}	3.1269(16)	177.19(16)	79.66(17)
S1... Br7 ^{vii}	3.1686(14)	170.17(15)	110.52(16)
S1... Br11 ^{vii}	3.0987(16)	177.54(13)	113.62(18)

Symmetry codes: i) $(1-x, -1/2+y, 1+z)$; ii) $(x, y, 1+z)$; iii) $(1-x, 1/2+y, 1-z)$; iv) $(-x, -1/2+y, 1-z)$; v) $(1-x, -1/2+y, 1-z)$; vi) $(1-x, -1/2+y, 2-z)$; vii) $(-1+x, y, z)$.

The geometric characteristics of most of the halogen bonds between tetrabromomethane and zinc-coordinated thiocyanate are close to those involving metal-free pseudohalide anions. Specifically, the average value of twelve crystallographically independent interatomic $\text{Br}\cdots\text{S}$ separations of 3.24 ± 0.10 Å in the $(\text{Bu}_4\text{N})_2[\text{Zn}(\text{NCS})_4]\cdot\text{CBr}_4$ co-crystals is nearly identical to the average $\text{Br}\cdots\text{S}$ distances of 3.22 ± 0.06 Å and 3.22 ± 0.01 Å in the reported co-crystals of CBr_4 with $(\text{Pr}_4\text{N})\text{NCS}$ and $(\text{Bu}_4\text{N})\text{NCS}$ salts, respectively.^{8,12} The average $\text{C-Br}\cdots\text{S}$ angles of 173 ± 6 deg, 171 ± 1 deg and 169 ± 3 deg, as well as the average $\text{C-S}\cdots\text{Br}$ angles of 110 ± 16 deg, 107 ± 8 deg and 107 ± 11 deg in the $(\text{Bu}_4\text{N})_2[\text{Zn}(\text{NCS})_4]\cdot 3\text{CBr}_4$, $2((\text{Pr}_4\text{N})\text{NCS})\cdot\text{CBr}_4$ and $(\text{Bu}_4\text{N})\text{NCS}\cdot\text{CBr}_4$ co-crystals, respectively, are also similar.

Overall, halogen bonding of zinc(II) tetrathiocyanate and tetrabromomethane produces a honeycomb-like network (Figure 4). The channels of this network are filled with Bu_4N^+

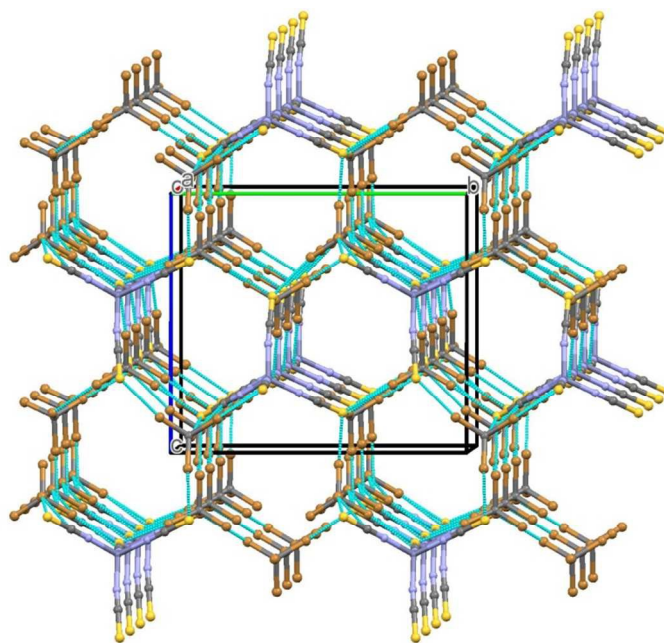


Figure 4. 3D-honeycomb network in the $(\text{Bu}_4\text{N})_2[\text{Zn}(\text{NCS})_4]\cdot 3\text{CBr}_4$ co-crystals in which halogen bonds are shown as blue lines and Bu_4N^+ cations are omitted for clarity. (Note: the view along c axes and details of the network are shown in Figures S1 – S3 in the ESI).

counterions (see Figure S3 in the ESI). This 3D-network comprises three types of (roughly) tetrahedral nodes, i.e. zinc ions, carbons (from the CBr_4 molecules), and sulfur atoms.²⁰ In particular, zinc ions form four coordination bonds with thiocyanate anions, which are aligned along the extensions of the Zn-N bonds (Zn-N-C angles vary from 171 to 177 deg). The sp^3 -hybridized carbon atoms of the CBr_4 molecules form four covalent C-Br bonds, and their bromine substituents are halogen-bonded with the sulfur ends of thiocyanates. Sulfur atoms represent the third type of node. They are connected to the zinc nodes via the combination of S-C and C-N covalent bonds and N-Zn coordination bonds. In addition, sulfur atoms are linked to the carbon nodes via combinations of $\text{S}\cdots\text{Br}$ halogen and Br-C covalent bonds. Notably, while C- $\text{S}\cdots\text{Br}$ angles vary in a rather wide range (Table 1), their average value of 110 deg is close to those for the carbon and zinc nodes.

Consideration of the X-ray structure of the $(\text{Bu}_4\text{N})_2[\text{Zn}(\text{NCS})_4]\cdot 3\text{CBr}_4$ co-crystals also revealed one unusual type of halogen bonding. Indeed, Figure 3 shows that the $\text{Zn}(\text{NCS})_4^{2-}$ complex is involved in twelve halogen bonds. Ten of these bonds link its thiocyanate ligands to ten different CBr_4 molecules. The remaining pair of halogen bonds (namely, $\text{S2}\cdots\text{Br1}$ and $\text{S1}\cdots\text{Br3}$) take place between two NCS^- ligands of the $\text{Zn}(\text{NCS})_4^{2-}$ complex and two bromine substituents of the same tetrabromomethane. In other words, the $\text{Zn}(\text{NCS})_4^{2-}$ complex and the top CBr_4 molecule in Figure 3 are connected via two-point halogen bonding (Figure 5).²¹

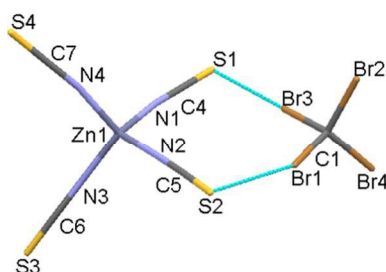


Figure 5. Two-point halogen bonding between the $[\text{Zn}(\text{NCS})_4]^{2-}$ complex and the CBr_4 molecule in the $(\text{Bu}_4\text{N})_2[\text{Zn}(\text{NCS})_4]\cdot 3\text{CBr}_4$ co-crystals. (Note: CBr_4 molecule is at equivalent position $(-x, -1/2+y, 1-z)$).

The distinct nature of this two-point halogen bonding brings about significant deviations of the geometric characteristics of the $\text{S2}\cdots\text{Br1}$ and $\text{S1}\cdots\text{Br3}$ contacts from those measured for the other halogen bonds in this system. For example, the data in the last column in Table 1 indicate that most of the $\text{C-S}\cdots\text{Br}$ angles measured in these co-crystals are between 97 to 128 deg, i.e. they are approximately in the same range as those observed in the halogen-bonded associates of bromocarbons with the isolated thiocyanate anions.^{8,12} For the $\text{S2}\cdots\text{Br1}$ and $\text{S1}\cdots\text{Br3}$ contacts, however, these angles are lower than 80 deg. The related C1-Br1-S2 angle of 158.9 deg, which characterizes one of these contacts, also deviates markedly from linearity. This divergence of the geometric features of the relatively soft intermolecular $\text{Br}\cdots\text{S}$ halogen bonding is apparently related to the constraints imposed by the other constituents of this two-point bonded structure.

Specifically, the fragment comprising the zinc ion with the two NCS ligands and the carbon atom with two bromine substituents that are involved in this two-point halogen bonding is nearly planar (Figure 5). In view of the tetrahedral geometries of $[\text{Zn}(\text{NCS})_4]^{2-}$ complex and CBr_4 electrophile, the $\text{Br}_3\text{-C}_1\text{-Br}_1$ and $\text{N}_1\text{-Zn-N}_2$ angles are about 110 deg and two Zn-NCS sides of this fragment are almost linear (vide supra). These rather rigid features lead to the relatively low $\text{C-S}\cdots\text{Br}$ angles and significant deviation of one of the $\text{C-Br}\cdots\text{S}$ bonds from linearity (if both $\text{C-Br}\cdots\text{S}$ bonds in this fragment were close to 180 deg, as is typical for halogen bonding, the $\text{C-S}\cdots\text{Br}$ angles would be about 70 deg, since the sum of the angles in the planar quadrilateral figure is 360 deg).

To clarify the preferable modes of intermolecular interaction between zinc tetrathiocyanate and tetrabromomethane, we carried out DFT computations of their associates (see Computational methods for details). Unrestricted optimizations of $\text{Zn}(\text{NCS}_4)^{2-}\cdot\text{CBr}_4$ dyads produced two distinct local minima both in the gas phase and in dichloromethane (the latter were carried out using PCM model with $\epsilon = 8.93$). Their structures correspond to two-point and three-point-bonded complexes (Figure 6). Notably, no minimum structure in which zinc tetrathiocyanate is linked to tetrabromomethane via common (one-point) halogen bond (similar to those which prevail in their co-crystals) was found regardless of the starting geometry of the pair.

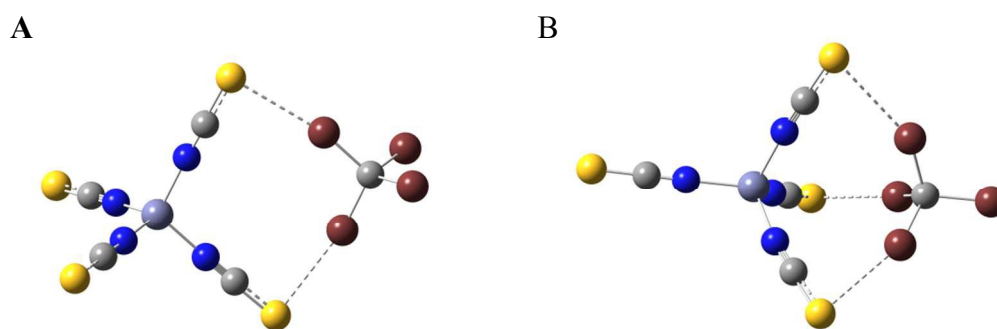


Figure 6. Two-point (A) and three-point (B) bonded intermolecular $[\text{Zn}(\text{NCS})_4]^{2-}\cdot\text{CBr}_4$ associates resulted from the DFT computations. Halogen $\text{Br}\cdots\text{S}$ bonds are shown as light dashed lines

Average values of S...Br distances, as well as C-Br...S and C-S...Br angles measured in these structures together with the characteristics of CBr₄·NCS associates are listed in Table 2.

Table 2. Geometric characteristics of the halogen bonds^a and interaction energies in the halogen-bonded associates of CBr₄ with [Zn(NCS)₄]²⁻ and NCS⁻ halogen-bond acceptors.

XB-acceptor	N ^b	d _{Br...S} , Å	∠C-Br...S, deg	∠C-S...Br, deg	ΔE, ^c kcal/mol	-ΔE/N, ^d kcal/mol
Calculated in the gas phase						
NCS ⁻	1 ^e	2.93	179	100	-10.9	10.9
[Zn(NCS) ₄] ²⁻	2 ^e	3.29	168	85	-10.6	5.3
[Zn(NCS ₄)] ²⁻	3 ^e	3.60	154	73	-10.7	3.6
NCS ⁻	1 ^{f, g}	2.87	179	98	-12.2	12.2
[Zn(NCS) ₄] ²⁻	2 ^f	3.24	169	83	-12.0	6.0
[Zn(NCS) ₄] ²⁻	3 ^f	3.46	157	72	-12.1	4.0
Calculated in dichloromethane						
NCS ⁻	1 ^e	3.23	179	95	-2.9	2.9
[Zn(NCS) ₄] ²⁻	2 ^e	3.41	169	81	-3.9	1.9
[Zn(NCS) ₄] ²⁻	3 ^e	3.71	153	72	-4.8	1.6
Experimental (from X-ray structures)						
NCS	1 ^h	3.22	170	104	-	-
[Zn(NCS) ₄] ²⁻	1 ⁱ	3.24	175	116	-	-
[Zn(NCS) ₄] ²⁻	2	3.27	168	79	-	-

a) For the two- and three-point bonded complexes, average values of distances and angles. b) Number of Br...S contacts in the single-point (N=1), two-point (N=2) and three-point (N=3) bonded CBr₄·[Zn(NCS)₄]²⁻ adducts. c) ΔE = E_{complex} - [E_{CBr4} + E_{Zn(NCS)4}] + BSSE, where E_{complex}, E_{CBr4} and E_{Zn(NCS)4} are sums of the electronic and zero-point energies, and BSSE is a basis set superposition error, see Supporting Information for details; d) Interaction energy per contact; e) Computations with the ωB97XD functional; f) Computations with the M062X functional; g) Data from ref. 12. h) Average values from the co-crystals of CBr₄ with (Pr₄N)NCS and (Bu₄N)NCS salts.^{8,12} i) Average from 10 independent contacts. j) Average from 2 contacts.

The data in Table 2 indicate that the C-Br...S and C-S...Br angles in the calculated two-point-bonded complexes are rather close to the C1-Br1...S2 and C5-S2...Br1 angles in the two-point halogen bonded fragment measured in the (Bu₄N)₂[Zn(NCS)₄]·3CBr₄ co-crystals. Also, in accordance with the previous studies of halogen bonding between CBr₄ and the separate

thiocyanate anion,¹² intermolecular Br \cdots S contacts in the CBr₄·[Zn(NCS)₄]²⁻ adduct resulting from the DFT computations in the gas phase were shorter than the corresponding separation in the complexes calculated in dichloromethane. Most notably, the interatomic separations, $d_{\text{Br}\cdots\text{S}}$, are gradually increasing, while C-Br \cdots S and C-S \cdots Br angles are decreasing as the mode of interaction changes from one-point bonding (in NCS⁻·CBr₄ dyads) to two- and three-point bonding in the CBr₄·[Zn(NCS)₄]²⁻ associates regardless of the media and the functional. The interaction energies, ΔE , of the two- and three-point halogen bonding in the CBr₄·[Zn(NCS)₄]²⁻ pairs in the gas phase are very close to those in the corresponding CBr₄·NCS⁻ complexes.²² Interactions energies in two- and three-point bonded complexes resulted from the computations in dichloromethane are only slightly stronger than that of the one-point bonded associate. Accordingly, the interaction energy per contact, $-\Delta E/N$, is decreasing from one- to two- and to three-point bonded pairs, in accordance with the increase of the interatomic separations.

The larger interatomic distances and weaker (per contact) interactions in the CBr₄·[Zn(NCS)₄]²⁻ associates are apparently related to the deviations of the C-Br \cdots S and C-S \cdots Br angles from the values optimal for halogen bonding. Indeed, consideration of the geometries of the calculated CBr₄·[Zn(NCS)₄]²⁻ associates indicate that two- and three-point halogen bonding results in small distortions of the tetrahedral geometries of their CBr₄ and [Zn(NCS)₄]²⁻ fragments.²³ As such, the formation of their two- and three-point bonded associates requires the deviations of the geometries of halogen bonds from their optimal values (vide supra). The variations of the energies of the halogen bonded complexes between CBr₄ and thiocyanate anion on the interatomic Br \cdots S distances, as well as C-Br \cdots S and C-S \cdots Br angles are shown in Figure 7.

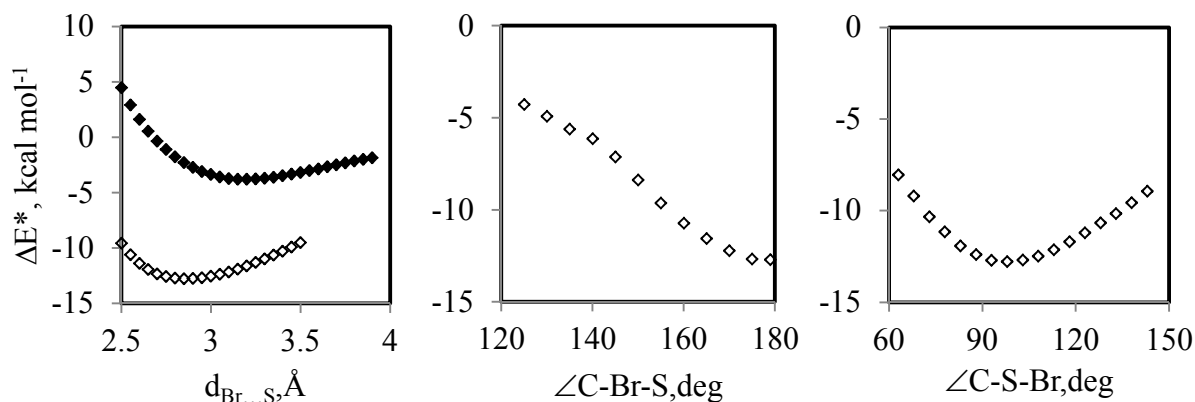


Figure 7. Dependencies of the interaction energies of the calculated halogen-bonded $\text{CBr}_4 \cdot \text{NCS}^-$ complexes, ΔE^* (as compared to the sum of the energies of the separate CBr_4 and NCS^-) on $\text{Br} \cdots \text{S}$ separation, as well as $\text{C-Br} \cdots \text{S}$ and $\text{C-S} \cdots \text{Br}$ angles (\diamond - in the gas phase, \blacklozenge - in CH_2Cl_2)

Noticeable, all the dependencies in Figure 7 are characterized by rather shallow minima. Still, significant deviation of the angles from the optimal values (especially decrease of the $\text{C-S} \cdots \text{Br}$ angles) results in substantial increase of the energy of the complex. Thus, the increase in the number of contacts in two- and three-point bonded complexes (which result in such a decrease of the $\text{C-S} \cdots \text{Br}$ angles) is offset by the decrease in the strength of the individual halogen bonds.

Conclusions.

The results of this work demonstrate that combination of coordination and halogen bonding of multidentate thiocyanate anions facilitates formation of hybrid 3D-networks comprising anionic zinc tetrathiocyanate complexes and neutral tetrabromomethane molecules. X-ray structural analysis as well as DFT computations showed that these halogen-bond donor and acceptor may form one-, two-, and three-point halogen bonds. It is noticeable, however, that while minimum-energy structures calculated for the $\text{CBr}_4 \cdot [\text{Zn}(\text{NCS})_4]^{2-}$ dyad correspond to two- and three-point-

bonded complexes, the $(\text{Bu}_4\text{N})_2 [\text{Zn}(\text{NCS})_4] \cdot 3\text{CBr}_4$ co-crystals comprise mostly one-point (and one two-point) halogen bonds.²⁴

In general, the multicenter interactions between chemical species lead to their strong and selective binding and facilitate molecular recognition and other applications, as was illustrated for several halogen-bonded systems.²⁵ Yet, the strength of the multipoint interactions between zinc tetrathiocyanate and tetrabromomethane is close to that of the one-point halogen bond. The lack of enhancement of the strength of the multicenter bonding for this pair is apparently related to the fact that the increase in the number of halogen bonds in the $\text{CBr}_4 \cdot [\text{Zn}(\text{NCS})_4]^{2-}$ dyad is offset by the deviations of the geometric characteristics of the individual contacts from their optimal values. As such, the one-point interactions of bromine substituents of the CBr_4 with thiocyanate anions from different $[\text{Zn}(\text{NCS})_4]^{2-}$ (which does not involve distortion of the optimal geometry of the halogen bond) is energetically more favorable than two- or three-point bondings. Accordingly, such one-point bonds prevail in the solid state structures.

Finally, the precise fit between geometries of the halogen-bond donors and acceptors which is required for the strong multicenter bonding between metal complexes and polybromosubstituted aliphatic electrophiles further underscores the high directionality of halogen bonding and its high potential for molecular recognition. The development of such fitting (key and lock) pairs is under study now.

Experimental section

Commercially available tetrabromomethane was purified by sublimation. $\text{Zn}(\text{NCS})_2$ was synthesized via reaction of $\text{Zn}(\text{NO}_3)_2 \cdot 6\text{H}_2\text{O}$ with KSCN as described earlier.²⁶

To synthesize $(\text{Bu}_4\text{N})[\text{Zn}(\text{NCS})_4]$, a solution of $\text{Zn}(\text{NCS})_2$ (1.94 g, 10.7 mmol) in acetone was added to a solution of $(\text{Bu}_4\text{N})\text{NCS}$ (6.42 g, 21.4 mmol) in acetone. A small amount of white

solid was filtered off and the solvent was removed on a rotary evaporator to afford a mixture of white solid and oil. This mixture was dissolved in dichloromethane and the insoluble material was filtered off. The evaporation of the solvent afforded colorless oil, which was dissolved in methanol. After this solution was stored in refrigerator (-30°C) for two days, (Bu₄N)₂[Zn(NCS)₄] precipitated as a white crystalline material. Yield 4.68 g (56%). mp 57 - 60 °C. FT-IR, ν_{\max} (cm⁻¹) 2963, 2876, 2076, 1470, 1379, 739. Anal. Calcd for C₃₆H₇₂N₆S₄Z: C, 55.25, H, 9.27, N, 10.74. Found C, 55.49, H, 9.34, N, 10.48.

To prepare a single crystal of halogen-bonded associate between [Zn(NCS)₄]²⁻ and CBr₄ suitable for X-ray measurements, (Bu₄N)[Zn(NCS)₄] (0.078 g, 0.10 mmol) and CBr₄ (0.100 g, 0.30 mmol) were dissolved in 4 mL of CH₂Cl₂ in a Schlenk tube. The resulting solution was carefully layered with of a 1:1 CH₂Cl₂/ hexane mixture (~2 mL), and then with hexane (20 mL), and kept in a refrigerator at -30 °C. Slow diffusion of hexane into the dichloromethane resulted in the formation of colorless rod-like crystals suitable for single-crystal X-ray crystallography.

X-ray measurements were made on a APEX-II CCD using Mo K α radiation (λ = 0.71073 Å) at 100(2) K. The structures were solved by direct methods and refined by full matrix least-squares treatment, and intermolecular contacts were analyzed using OLEX2 structure solution, refinement and analysis program.²⁷ CCDC 1421337 contain the supplementary crystallographic data for this paper. These data can be obtained free of charge from the Cambridge Crystallographic Data Centre via www.ccdc.cam.ac.uk/data_request/cif.

Crystal data: (Bu₄N)₂ [Zn(NCS)₄]·3CBr₄. C₃₉H₇₂Br₁₂N₆S₄Zn, M = 1777.56, monoclinic, a = 13.6976(7) Å, b = 16.1004(8) Å, c = 14.1055(7) Å, β = 92.642(2)°, U = 3107.5(3) Å³, T = 100.01, space group P2₁ (no. 4), Z = 2, μ (MoK α) = 8.277, 106128 reflections measured, 18264 unique (R_{int} = 0.0896) which were used in all calculations. The final $wR(F_2)$ was 0.0851 (all data).

The details of the UV-Vis measurements and the calculations of the formation constants were described previously.^{12,28} It should be noted however, that, in contrast to the systems with the separate anions, calculation of the accurate formation constants of the halogen-bonded associates involving metal-coordinated anions were hindered by two factors. First, the absorption bands of the $\text{CBr}_4 \cdot [\text{Zn}(\text{NCS})_4]^{2-}$ complex are blue-shifted as compared to those of the $\text{CBr}_4 \cdot \text{NCS}^-$ dyad (vide supra). As such, the absorption bands of the formers are overshadowed by the absorption of the components, which complicated the intrinsically difficult (due to their low values) determination of the formation constants of the complexes with the metal-coordinated anions. Second, in the solutions with the high concentrations of components (which are necessary to measure low equilibrium constants), Benesi-Hildebrand dependencies and regression analysis showed significant deviations from the linearity. This implies that besides 1:1 complexes, 2:1 or 1:2 associates are also formed. In fact, the measurements of the stoichiometry of the complex via Job's method produced a very broad maximum between 1:1 and 1:2 complexes. As such, an approximate value of the formation constant for the $\text{CBr}_4 \cdot [\text{Zn}(\text{NCS})_4]^{2-}$ associate of $K = 0.8 \text{ M}^{-1}$ was obtained from the linear parts of the Benesi-Hildebrand and least-square deviations treatments.

Quantum-mechanical calculations were carried out using the Gaussian 09 suite of programs.²⁹ Geometries of halogen-bonded $\text{CBr}_4 \cdot [\text{Zn}(\text{NCS})_4]^{2-}$ associates were optimized without constraints in the gas phase and in dichloromethane *via* DFT calculations with MO6-2X and wB97XD functionals.³⁰ In our earlier studies, these methods most accurately reproduced experimental characteristics of the complexes between bromosubstituted electrophiles and halide and pseudohalide anions.^{12,28} Recent theoretical study also demonstrated that they provide the best (among DFT and MP2 ab initio methods) characteristics of the halogen-bonded complexes with

anionic halogen-bond acceptors (e.g. Cl^- and Br^-).²⁷ 6-311+G(d,p) basis set was used for all atoms except iodine, for which 6-311G* basis set was downloaded from EMSL Basis Set Exchange Library.^{31,32} Geometry optimizations in dichloromethane were carried out using the polarizable continuum model (PCM).³³ Energies and atomic coordinates of optimized species are listed in ESI. The energies of interaction were determined by subtracting the sum of the energies of isolated CBr_4 and $[\text{Zn}(\text{NCS})_4]^{2-}$ species from the energy of the $\text{CBr}_4 \cdot [\text{Zn}(\text{NCS})_4]^{2-}$ associates and adding basis set superposition error (BSSE): $\Delta E = E_{\text{complex}} - [E_{\text{CBr}_4} + E_{\text{Zn}(\text{NCS})_4}] + \text{BSSE}$, where E_{complex} , E_{CBr_4} and $E_{\text{Zn}(\text{NCS})_4}$ are sums of the electronic and zero-point energies). The BSSE values were determined via the counterpoise method.³⁴ Zero-point energies (ZPE) and thermal corrections were taken from unscaled vibrational frequencies.

The dependencies of the energies of the calculated $\text{CBr}_4 \cdot \text{NCS}^-$ complexes on the interatomic separations and bond angles were calculated using Opt=ModRedundant option in Gaussian 09.²⁹ During these computations, $\text{Br} \cdots \text{S}$ separation or $\text{C}-\text{Br} \cdots \text{S}$ or $\text{C}-\text{S} \cdots \text{Br}$ angles were fixed at certain value, and the other coordinates were optimized. Interaction energies of such complexes, ΔE^* , were calculated by subtraction energies of the separate CBr_4 and NCS^- anion from the energy of the complex.

Acknowledgements. We thank Maria Sholola for the assistance with the UV-Vis spectral measurements and the National Science Foundation (grant CHE-1112126) for financial support.

References and Notes

- 1) a) C. Janiak, *J. Chem. Soc. Dalton Trans.* 2003, 2781. b) C. Hendon, D. Tiana, A. Walsh, *Phys. Chem. Chem. Phys.*, 2012, **14**, 13120. c) E. Coronado, G. M. Espallargas, *Chem. Soc. Rev.* 2013, **42**, 1525. d) H.L. Jiang, T. Makal, H.-C. Zhou, *Chem. Soc. Rev.* 2013, **257**, 2232.
- 2) P. Silva, S.M.F. Vilela, J.P.C. Tome, F.A. Almeida Paz, *Chem. Soc. Rev.*, 2015 **44**, 6774.
- 3) (a) R. Bertani, P. Sgarbossa, A. Venzo, F. Lejl, M. Amati, G. Resnati, T. Pilati, P. Metrangolo, G. Terraneo, *Coord. Chem. Rev.* 2010, **254**, 677. (b) P. Metrangolo, H. Neukirch, T. Pilati and G. Resnati, *Acc. Chem. Res.*, 2005, **38**, 386. (c) P. Metrangolo, F. Meyer, T. Pilati, G. Resnati and G. Terraneo, *Angew. Chem., Int. Ed.* 2008, **47**, 6114. (d) A. Priimagi, G. Cavallo, P. Metrangolo, G. Resnati, 2013, **46**, 2686.
- 4) (a) K. Rissanen, *CrystEngComm*, 2008, **10**, 1107. (c) L. C. Gilday, S. W. Robinson, T.A. Barendt, M.J. Langton, B. R. Mullaney, P.D. Beer, *Chem. Rev.* 2015, **115**, 7118.
- 5) (a) K. Bowman-James, A. Bianchi, E. Garcia-Espana, *Anion Coordination Chemistry*, Wiley VCH, Weinheim, 2011. (b) J. Ribas, A. Escuer, M. Monfort, R. Vicente, R. Cortes, L. Lezama, T. Rojo, *Coord. Chem. Rev.*, 1999, **193-195**, 1027. (c) W.P. Fehlhammer, W. Beck, *Z. Anorg. Allg. Chem.*, 2013, **639**, 1053.
- 6) (a) L. Tchertanov, *Supramol. Chem.*, 2000, **12**, 67. (b) L. Tchertanov, C. Pascard, *Acta Crystallogr. B*, 1997, **B53**, 904. (c) L. Tchertanov and C. Pascard, *Acta Crystallogr. B*, 1996, **B52**, 685. d) I. S. Bushmarinov, O. G. Nabiev, R. G. Kostyanovsky, M. Yu. Antipin, K.A. Lyssenko, *CrystEngComm*, 2011, **13**, 2930.
- 7) (a) H. Bock, S. Holl, *Z. Naturforsch. B*, 2002, **57**, 835. (b) H. Bock, S. Holl, *Z. Naturforsch. B*, 2002, **57**, 713.

- 8) (a) S.V. Rosokha, I.S. Neretin, T.Y. Rosokha, J. Hecht and J.K. Kochi, *Heteroat. Chem.*, 2006, **17**, 449. (b) S.V. Rosokha and J.K. Kochi, in *Halogen Bonding: Fundamentals and Applications*, ed. P. Metrangolo and, G. Resnati, Springer, Berlin, 2008, p. 137.
- 9) M. Formigue, P. Auban-Senzier, *Inorg. Chem.*, 2008, **47**, 9979.
- 10) P. Cauliez, V. Polo, T. Roisnel, R. Llusar, M. Fourmigue, *CrystEngComm*, 2010, **12**, 558.
- 11) J. Viger-Gravel, I. Korobkov, D.L. Bryce, *Cryst. Growth Des.*, 2011, **11**, 4984. (b)
- 12) S. V. Rosokha, C.L. Stern, A. Swartz, R. Stewart, *Phys. Chem. Chem. Phys.* 2014, **16**, 12968.
- 13) (a) L. Brammer, G.M. Espallargas, S. Libri, *CrystEngComm*, 2008, **10**, 1712. (b) F. Zordan, L. Brammer, P. Sherwood, *J. Am. Chem. Soc.*, 2005, **127**, 5979. (c) G. M. Espallargas, L. Brammer, P. Sherwood, *Angew. Chem., Int. Ed.* 2006, **45**, 435. (d) J. Ormond-Prout, P. Smart, L. Brammer, *Cryst. Growth Des.*, 2012, **12**, 205.
- 14) (a) S.V. Rosokha, M. K. Vinakos, *Cryst. Growth Des.*, 2012, **12**, 4149. (b) S. V. Rosokha, J. J. Lu, T.Y. Rosokha, J. K. Kochi, *Chem. Commun.*, 2007, 3383.
- 15) F.F. Awwadi, D. Taher, S. F. Haddad, M. M. Turnbull, Mark M. *Cryst. Growth Des.*, 2014, **14**, 1961.
- 16) (a) H. Hartl, S. Steidl, *Z. Naturforsch., B: Chem. Sci.* 1977, **32**, 6. (b) H. Hartl, S. Steidl *Acta Cryst., B: Struct. Crystallogr. Cryst. Chem.* 1980, **36**, 65 (c) L. R. Nassimbeni, M. L. Niven, A. P. Suckling, *Inorg. Chim. Acta*, 1989, **159**, 209.
- 17) (a) J. E. Ormond-Prout, P. Smart, L. Brammer, *Cryst. Growth Des.*, 2012, **12**, 205. (b) K. Herve, O. Cador, S. Golhen, K. Costuas, J.-F. Halet, T. Shirahata, T. Muto, T. Imakubo, A. Miyazaki, L. Ouahab, *Chem. Mater.* 2006, **18**, 790. (c) A. Pramanik, G. Das *Polyhedron*, 2010, **29**, 2999. (d) R. G. Surbella III, C. L. Cahill, *CrystEngComm*, 2014, **16**, 2352. (e) L.

Rajput, K. Biradha, *CrystEngComm*, 2009, *11*, 1220. (f) J. Gong, X. He, L. Chen, X. Shen, D. Zhu, *J. Coord. Chem.* 2013, **66**, 2875.

- 18) For example, HOMO energies of $\text{Zn}(\text{NCS})_4^{2-}$ and NCS^- anions are -7.87 eV and -7.52 eV, respectively, and HOMO energies of ZnBr_4^{2-} and Br^- anions are -8.18 eV and -7.95 eV, respectively (DFT computations with ωB97XD functional in dichloromethane).
- 19) A. Bondi, *J. Phys. Chem.*, 1964, **68**, 441.
- 20) Due to close to tetrahedral geometry of its nodes, the grid in Figure 4 resembles diamondoid network. Yet, the presence of the fragments involving two-point halogen-bonding (shown in Figure 5 and Figure S2) precludes description of $\text{CBr}_4 \cdot [\text{Zn}(\text{NCS})_4]^{2-}$ network as diamondoid.
- 21) Several other examples of two-point halogen bonding were reported recently, see: a) D. Cao, M. Hong, A.K. Blackburn, Z. Liu, J.M. Holcroft, J. F. Stoddart, *Chem. Sci.* 2014, **5**, 4242. (b) S. M. Oburn, N. P. Bowling, E. Bosch, *Cryst. Growth Des.* 2015, **15**, 1112. (c) S.V.Rosokha, E.A.Loboda, *J. Phys. Chem.*, 2015, **119**, 3833. (d) S. H. Jungbauer, S. Schindler, E. Herdtweck, S. Keller, S. M. Huber, *Chem. Eur. J.*, 2015, **21**, 13625.
- 22) Although it could be expected that coordination of thiocyanate anions to the Zn^{2+} dication would decrease electron density on their sulfur atoms, and thus strength of the halogen bond with CBr_4 , actually, the surface electrostatic potentials (ESP) of the zinc-coordinated thiocyanate are slightly more negative than those of the separate anion. Specifically, for the coordinated NCS^- anion, ESP on the sulfur atom surface varies from about -110 kcal mol⁻¹ along the extension of the C-S bond to -125 kcal mol⁻¹ in the direction perpendicular to C-S bond, while the corresponding values calculated for the separate NCS^- anion are 95 kcal mol⁻¹ and 112 kcal mol⁻¹ (calculated at isovalue 0.0004, see Figure S4 in ESI).

- 23). Specifically, the halogen-bonded thiocyanate ligands of $[\text{Zn}(\text{NCS})_4]^{2-}$ are slightly bent toward CBr_4 and vice versa. For example, the thiocyanate ligand, which does not participate in the halogen bonding of the two-point-bonded $\text{CBr}_4 \cdot [\text{Zn}(\text{NCS})_4]^{2-}$ complex (resulted from the DFT computations with ωB97XD functional in the gas phase), is aligned along the extension of the Zn-N bond, such that the Zn-N-S angle is 179 deg. In comparison, halogen-bonded NCS^- ligands deviate toward CBr_4 , so that the corresponding Zn-N-S angles are, on average, about 178 deg. Similarly, the angles between carbon bonds with bromine atoms that do not participate in halogen bonding are about 1.8 deg larger than those between carbon bonds with the two halogen-bonded bromines. The distortions of the geometries of zinc tetrathiocyanate and tetrabromomethane in the other two- and three-point bonded complexes are similar.
- 24) It should be noted however, that the conclusion about the preference of the one-point bonding in the solid state is based currently only on the X-ray structure of the $(\text{Bu}_4\text{N})_2 [\text{Zn}(\text{NCS})_4] \cdot 3\text{CBr}_4$ co-crystals.
- 25) (a) S. H. Jungbauer, D. Bulfield, F. Kniep, C. Lehmann, E. Herdtweck, S. M. Huber, *J. Am. Chem. Soc.*, 2014, **136**, 16740. (b) B. R. Mullaney, B.E. Partridge, P.D. Beer, *Chem.- Eur. J.* 2015, **221**, 1660. (c) R. Tepper, B. Schulze, M. Jaeger, C. Friebe, D.H. Scharf, H. Goerls, U.S. Schubert, *J. Org. Chem.*, 2015, **80**, 3139.
- 26) M. Montazerzohori, S. A. Musavi, *J. Coord. Chem.*, 2008, **61**, 3934.
- 27) (a) G.M. Sheldrick, SHELXTL Version 6.14; Bruker Analytical X-ray Instruments, Inc.: Madison, WI, 2003. (b) O.V. Dolomanov, L.J. Bourhis, R.J. Gildea, J.A.K. Howard and H.J. Puschmann, *Appl. Cryst.*, 2009, **42**, 339.
- 28) S. V. Rosokha, C. L. Stern and J.T. Ritzert, *Chem.- Eur. J.* 2013, **19**, 8774.

- 29) Gaussian 09, Revision C.01, M. J. Frisch, G. W. Trucks, H. B. Schlegel, G. E. Scuseria, M. A. Robb, J. R. Cheeseman, G. Scalmani, V. Barone, B. Mennucci, G. A. Petersson, H. Nakatsuji, M. Caricato, X. Li, H. P. Hratchian, A. F. Izmaylov, J. Bloino, G. Zheng, J. L. Sonnenberg, M. Hada, M. Ehara, K. Toyota, R. Fukuda, J. Hasegawa, M. Ishida, T. Nakajima, Y. Honda, O. Kitao, H. Nakai, T. Vreven, J. A. Montgomery, Jr., J. E. Peralta, F. Ogliaro, M. Bearpark, J. J. Heyd, E. Brothers, K. N. Kudin, V. N. Staroverov, R. Kobayashi, J. Normand, K. Raghavachari, A. Rendell, J. C. Burant, S. S. Iyengar, J. Tomasi, M. Cossi, N. Rega, J. M. Millam, M. Klene, J. E. Knox, J. B. Cross, V. Bakken, C. Adamo, J. Jaramillo, R. Gomperts, R. E. Stratmann, O. Yazyev, A. J. Austin, R. Cammi, C. Pomelli, J. W. Ochterski, R. L. Martin, K. Morokuma, V. G. Zakrzewski, G. A. Voth, P. Salvador, J. J. Dannenberg, S. Dapprich, A. D. Daniels, O. Farkas, J. B. Foresman, J. V. Ortiz, J. Cioslowski, and D. J. Fox, Gaussian, Inc., Wallingford, CT, 2009.
- 30) (a) Y. Zhao and D.G. Truhlar, *Theor. Chem. Acc.*, 2008, **120**, 215. (b) J.-D. Chai, M. Head-Gordon, *Phys. Chem. Chem. Phys.*, 2008, **10**, 6615.
- 31) A. Bauza, I. Alkorta, A. Frontera and J. Elguero. *J. Chem. Theory Comput.*, 2013, **9**, 5201.
- 32) (a) M. N. Glukhovstev, A. Pross, M.P. McGrath, L. Radom, *J. Chem. Phys.*, 1995, **103**, 1878. (b) D. Feller, *J. Comp. Chem.*, 1996, **17**, 1571. (c) K.L. Schuchardt, B.T. Didier, T. Elsethagen, L. Sun, V. Gurumoorthi, J. Chase, J. Li, T.L. Windus, *J. Chem. Inf. Model.*, 2007, **47**, 1045.
- 33) J. Tomasi, B. Mennucci and R. Cammi, *Chem. Rev.*, 2005, **105**, 2999.
- 34) S. F. Boys and F. Bernardi, *Mol. Phys.*, 1970, **19**, 553.